Final-state correlation effects in Auger line shapes: Application to SiO$_2$

David E. Ramaker

Chemistry Department, George Washington University, Washington D.C. 20052
(Received 10 December 1979)

Final-state correlation effects in Auger line shapes are considered within the cluster linear combination of atomic orbitals–molecular orbitals–configuration interaction theory with a parametrized Hamiltonian. A model problem is solved analytically to elucidate the role of final-state hole-hole correlation and to understand the localization of the holes on rather small subclusters of the system. The relationship of the correlation effects to the relative magnitudes of the one-center hole-hole repulsion u and the bandwidth Γ has been previously reported; however, this previous work has been limited to metallic single element conductors. This work extends the theory to covalently bonded insulators (and possibly semiconductors) consisting of more than one element. Application of the theory is made to the O KVV and Si $L_{23}VV$ Auger line shapes from SiO$_2$. A high-energy shoulder at 511 eV in the O KVV line shape is interpreted as arising directly from correlation effects. A peak at 50 eV in the Si $L_{23}VV$ line shape, its intensity significantly underestimated by the previous theory, is now accounted for; a peak at 70 eV previously suggested to be a shake satellite is now indicated also to arise from correlation effects. Both line shapes reveal a density of states primarily localized on an Si$_2$O subcluster. The magnitude of the hole-hole repulsion on the subcluster and between neighboring Si$_2$O subclusters is empirically determined from the Auger line shapes to be ~ 11 and 4 eV, respectively. The oxygen $2p$ nonbonding bandwidth is estimated to be ~ 6 eV, but in light of other theoretical and experimental results, our result is believed to be 1–2 eV too large. Reasons for our overestimate are discussed.

I. INTRODUCTION

Recently we reported results of an investigation of the Auger line shapes involving the valence electrons in SiO$_2$.[1,2] In this work we compared the Si $L_1L_{23}VV$, the Si $L_{23}VV$, and O KLL experimental Auger line shapes with those predicted from theory. The electronic structure of SiO$_2$ for this work was described in terms of one-electron molecular orbitals (MO) on minimum-sized clusters (i.e., central atom plus nearest neighbors such as SiO$_4^{4-}$ and Si$_2$O^{6+} in SiO$_2$). The results of this comparison were gratifying, with the calculated and experimental Auger line shapes in generally good agreement in all three line shapes. Figure 1 summarizes these data. The only significant discrepancies are (1) the absence of the high-energy shoulder at 511 eV in the O KVV theoretical line shape and (2) the significant underestimation of the low-energy peak at 50 eV in the Si $L_{23}VV$ line shape.

That good agreement between the cluster linear combination of atomic orbitals–molecular orbitals (LCAO–MO) theory and experiment should be obtained is perhaps not surprising. The observed Auger line shapes in the more covalent SiO$_2$ are very similar to the corresponding line shapes in more ionic solids where the cluster LCAO–MO model is expected to be valid. Thus, for example, the S and P $L_{23}VV$ Auger line shapes obtained from the highly ionic Li salts are very similar in all aspects to the Si $L_{23}VV$ line shape.[3] Furthermore, the O KVV line shape from the more

ionic MgO is essentially identical to the O KVV line shape in SiO$_2$.[4] The valence electron energy levels for SiO$_2$ have been probed by photoemission, by Si $K\beta$ and $L_{2,3}$ x-ray emission, and by O $K\alpha$ x-ray emission.[5] These data have been well described within the SiO$_4^{4-}$ cluster one-electron LCAO–MO model[1]; indeed, in our work, the orbital energies were obtained from the XPS data and the LCAO–MO populations were adjusted to reproduce the XES data. Furthermore, the atomic Auger matrix elements giving the Auger intensity

$$|M_{cab}|^2 = \sum_l |\langle f_c kl | r_{12}^{-1} | f_a f_b \rangle|^2 \qquad (1)$$

(f_c and kl represent the original core-hole and final-state continuum functions, respectively; f_a and f_b, the two final-state holes in the Auger process) were not evaluated in our theory but were estimated from gas-phase Auger data.[2]

Despite these successes of the MO model, one can justifiably question the validity of utilizing the cluster one-electron MO model to study Auger transitions in covalent solids. The Auger process produces two final-state holes, whereas the x-ray emission and photoemission processes produce just one hole. In general, these two final-state holes see one another, a repulsive interaction U exists between them, and their relative motion is correlated. This interaction exhibits itself in the energy of the Auger electron

$$E_{cvv'} = E_c - E_v - E_{v'} - U_{vv'}, \qquad (2)$$
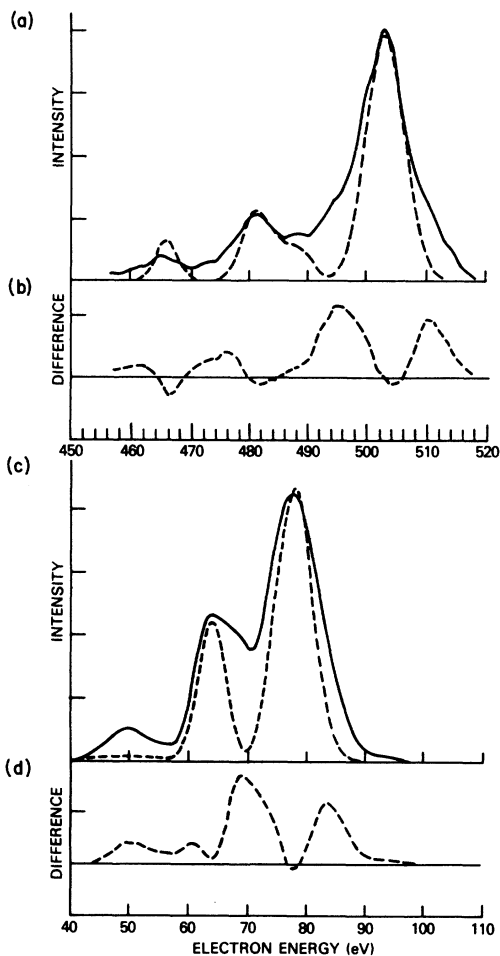
FIG. 1. (a) A comparison of the experimental (solid line) O KVV Auger line shape with the theoretical line shape determined previously (Ref. 1). (b) The difference between the experimental and calculated line shapes. The peaks at 475 and 495 eV have been identified to be shake satellites. The peak at 511 eV is the subject of this work. (c) A comparison of the experimental (solid line) Si $L_{23}VV$ Auger line shape with the theoretical line shape determined previously (Ref. 1). (d) The difference between the experimental and calculated line shapes. The peaks at 52 and 70 eV have been attributed to shake satellites, but in this work are shown also to arise partially from correlation effects. Possible sources of the peak at 84 eV are summarized elsewhere (Refs. 1, 27, 41, and 42).

where the E's are the one-electron binding energies of core and valence electrons, respectively. In SiO_2, U is substantial, varying from 5 to 20 eV depending on the central atom and the localized nature of the final states involved. Hole-hole correlation may also substantially alter the Auger intensities. We note that the hole-hole correlation effects on the intensities of a single atom are in some sense already included in our model

because the experimental atomic Auger matrix elements were utilized. Thus, only the interatomic correlation effects and banding effects are apparently absent in our earlier one-electron model.

In the one-electron model one can approximate U by a difference between two terms, the direct hole-hole Coulomb repulsion F and static relaxation term R; thus $U = F - R$. R accounts for the shift in the binding energy of one hole state orbital due to the presence of the other hole. In the MO model, F and R are expanded in the atomic equivalents

$$F_{vv'} = \sum_{ij} c_{vi}^2 c_{v'j}^2 F_{ij}^0 + \cdots, \tag{3}$$

$$R_{vv'} = \sum_{ij} c_{vi}^2 c_{v'j}^2 r_i \delta_{ij}, \tag{4}$$

where the F^0 are the atomic Slater integrals between atomic orbitals i and j, and r_i is an atomic intrashell relaxation energy, both defined previously.[1]

A problem with the cluster one-electron MO model is that F and R are cluster-size dependent. Both F and R go to zero as the cluster size increases. Thus the following question arises: What is the appropriate cluster size? In the one-electron band model for a solid, F and R are, of course, zero. This is merely consistent with the notion that the holes are completely free to roam about the solid or cluster, and hence are completely delocalized from one another. There is experimental evidence[6-8] that in some metallic solids, such as in Cu, Zn, and Ni, the final-state holes, even in the conduction band, are not free to roam about the solid, but are forced to remain on the atom in which they were created (the atom with the initial core hole). This is evident because the experimental Auger intensity does not reflect the density of states (DOS) of the band but rather exhibits multiplet structure consistent with an atomic model. Furthermore, the apparent magnitude of U is consistent with the hole-hole interaction one would expect if both holes were localized on the same atom.

Electron or hole-hole correlation in metallic solids has been considered within the context of the Hubbard[9] or Anderson[10] model. Within these models, Cini[11] and Sawatsky[12] have independently examined the role of electron correlation in metals and have attributed the behavior indicated above to hole-hole correlation. More specifically, if the one-center hole-hole interaction U is large compared to the bandwidth Γ, energy conservation forces the two holes to remain localized on the atom where they were created, producing an

Auger intensity consistent with the atomic model.

In this work we wish to consider hole-hole correlation within the cluster LCAO-MO-CI model (CI referring to configuration interaction) with a parametrized Hamiltonian. Electron correlation in molecules is normally considered within the context of configuration interaction theory. It has the advantage of being easily applied within the cluster model where the two-center Coulomb-repulsion integrals are easily included. More importantly, it can be easily applied to ionic and molecular insulators and more covalently bonded systems such as SiO_2, which may involve more than one element, and hence involve several different interaction energies. In Sec. II we summarize the general theory, providing working formulas for implementing the CI theory. To elucidate the effects of hole-hole correlation and attempt to understand why the one-electron cluster molecular orbital model may be adequate for interpreting Auger line shapes in some covalently bonded solids, we examine the role of CI mixing on a model problem.

In Sec. III we present numerical results appropriate for the O KVV and Si $L_{23}VV$ Auger line shape in SiO_2. An attempt is made to account for the two described discrepancies between the theoretical and experimental Auger line shapes. The effects of cluster size and the two-center Coulomb integrals are also examined.

II. CLUSTER LCAO-MO-CI THEORY WITH PARAMETRIZED HAMILTONIAN

A. General formulations

The LCAO-MO-CI theory and its application to molecules is well known.[13] We briefly summarize here the general formulations, also making the necessary definitions and indicating our approximations and limitations.

The molecular orbitals are constructed by a linear combination of atomic orbitals

$$\varphi_\mu = \sum_i c_{\mu i} f_i \tag{5}$$

in the usual manner, the coefficients determined from the solution of the secular equation

$$\sum_j (H_{ij} - \epsilon_\mu S_{ij}) c_{\mu j} = 0 . \tag{6}$$

The atomic orbitals f_i at this point are completely unspecified; they may be Slater-type atomic orbitals, Hartree-Fock atomic orbitals, or even symmetry adapted atomic orbitals involving more than one atomic center. They are specified through the choice of orbital matrix elements

$$H_{ii} = \langle f_i | \hat{h} | f_i \rangle = \alpha_i ,$$
$$H_{ij} = \langle f_i | \hat{h} | f_j \rangle = V_{ij} , \tag{7}$$
$$S_{ij} = \langle f_i | f_j \rangle = \delta_{ij} .$$

In this work, the matrix elements will be treated as parameters such as the tight-binding parameters in a band calculation[14]; that is, the α_i and V_{ij} are adjusted so that the resultant one-electron MO energy levels ϵ_μ and orbital populations $c_{\mu i}^2$ are similar to some previously determined one-electron DOS. We have reported previously our best estimates of the DOS and orbital populations in SiO_2.[1] They were determined from experimental data and *ab initio* cluster MO calculations.

The decision here to set the off-diagonal overlaps equal to zero is a matter of convenience for this model problem. In general, they are not zero; however, it has been shown[15] that by including them, one in effect scales the V_{ij}. Since our V_{ij} are parametrized anyway, the ultimate effect of ignoring the off-diagonal overlaps is minimal. We have discussed elsewhere[16] the effect of S_{ij} on the distribution of local versus bonding charge and the resultant effects on the Auger intensity. These effects are not important in this work.

Within the configuration interaction theory, we shall limit our considerations to filled bands. This means that all configurations describing the system after the Auger decay will have exactly two holes, and we can write the final-state wave function as a sum of the two-hole configurations,

$$\Psi_{vv'}(\vec{r}_1, \vec{r}_2) = \sum_{\alpha\beta} D_{vv',\alpha\beta} \varphi_\alpha(\vec{r}_1) \varphi_\beta(\vec{r}_2) . \tag{8}$$

Here, the $\varphi_\mu(\vec{r})$ are the molecular orbitals spanning the cluster as constructed above. The restriction to filled bands is a good approximation in an insulator such as SiO_2, as the unfilled conduction bands are approximately 10 eV above the filled valence bands, and thus an insignificant amount of configuration mixing between these two bands should occur for realistic conditions. This approximation becomes less applicable for semiconductors and metals where the band gap is small or zero.

The mixing coefficients $D_{vv',\alpha\beta}$ in Eq. (8) are determined by the secular equation

$$\sum_{\gamma\delta} (H_{\alpha\beta,\gamma\delta} - E_{vv'} S_{\alpha\beta,\gamma\delta}) D_{vv',\gamma\delta} = 0 , \tag{9}$$

where the full Hamiltonian now includes both one- and two-electron terms $\hat{H} = \hat{h}_1 + \hat{h}_2 + \hat{U}_{12}$. Consistent with Eq. (7), the matrix elements are

$$H_{\alpha\beta,\gamma\delta} = \langle \varphi_\alpha \varphi_\beta | \hat{H} | \varphi_\gamma \varphi_\delta \rangle$$

$$= \langle \varphi_\alpha | \hat{h}_1 | \varphi_\gamma \rangle \delta_{\beta\delta} + \langle \varphi_\beta | \hat{h}_2 | \varphi_\delta \rangle \delta_{\alpha\gamma} + U_{\alpha\beta,\gamma\delta}$$

$$\tag{10}$$

and

$$S_{\alpha\beta,\gamma\delta} = \delta_{\alpha\gamma} \delta_{\beta\delta} , \tag{11}$$

where

$$U_{\alpha\beta,\gamma\delta} = \langle \varphi_\alpha \varphi_\beta | \hat{U}_{12} | \varphi_\gamma \varphi_\delta \rangle$$

$$= \sum_{mn} c_{\alpha m} c_{\beta n} c_{\gamma m} c_{\delta n} u_{mn} . \tag{12}$$

In Eq. (12), the zero-differential-overlap (ZDO) approximation has been employed to reduce the two-center integrals $U_{\alpha\beta,\gamma\delta}$ to a sum of atomic Coulomb integrals u_{mn}. Throughout, we use the notation $\langle 12 | r_{12}^{-1} | 12 \rangle \equiv [1^2 | r_{12}^{-1} | 2^2]$ to indicate the two-electron integrals.

Those integrals involving two centers are evaluated using an approximation of Mataga and Nishimoto[17]

$$u_{mn} = e^2 [R_{mn} + 2e^2/(u_n + u_m)]^{-1} , \tag{13}$$

and the one-center integrals

$$u_n = [f_n^2 | r_{12}^{-1} | f_n^2] - r_n \tag{14}$$

are treated as parameters. In Eq. (13), R_{mn} is the internuclear distance between the two centers, and e is the charge on the electron. This approximation, found in many semiempirical MO programs, simply takes an appropriate average of two extrema; for large R_{nm}, $U_{mn} = e^2/R_{mn}$, for very small R_{mn}, $u_{mn} = (u_n + u_m)/2$, where u_n, u_m are the one-center integrals. r_n in Eq. (14) is the atomic static relaxation term as mentioned previously (see Eq. 4); the one-center Coulomb matrix element can be approximated from the tabulations of Mann.[18] In practice, we have treated u_n as a parameter observing hole-hole correlation effects as u_n is increased.

The Auger electron energy is now given in terms of the eigenvalues of Eq. (9),

$$E_{cvv'} = E_c - E_{vv'} , \tag{15}$$

in contrast with Eq. (2) which involved the one-electron MO energies. The Auger intensity now involves the two-hole DOS

$$I_{cvv'} = \sum_l |\langle f_c kl | r_{12}^{-1} | \Psi_{vv'}(\vec{r}_1, \vec{r}_2) \rangle|^2$$

$$= \left| \sum_{\alpha\beta} D_{vv',\alpha\beta} c_{\alpha a} c_{\beta b} \right|^2 |M_{cab}|^2 , \tag{16}$$

where we have inserted Eqs. (1), (5), and (8), and made the usual assumption that only the one-center Auger matrix elements are significant

(1). The indices "a" and "b" label atomic orbitals on the atom with the initial core hole; thus the Auger line shape reflects the two-hole local DOS. It is this feature which hastens the convergence of the cluster expansion result to the bulk limit and thus provides a reasonable probability for the success of the cluster expansion in this work.

The above analysis ignores the role of hole (electron) spin. Actually, the spin symmetry decreases the number of two-hole configurations which have to be included in the final-state wave function. Configurations of the "diagonal" type $\varphi_k \varphi_k$ only take the singlet form $\varphi_k \varphi_k 2^{-1/2}(\alpha\beta - \beta\alpha)$. Nondiagonal configurations can take both the singlet and the triplet forms, respectively:

$$2^{-1/2}(\varphi_k \varphi_l + \varphi_l \varphi_k) 2^{-1/2}(\alpha\beta - \beta\alpha) ,$$

$$2^{-1/2}(\varphi_k \varphi_l - \varphi_l \varphi_k) \times \begin{cases} 2^{-1/2}(\alpha\beta + \beta\alpha) \\ \alpha\alpha \\ \beta\beta \end{cases} .$$

Since singlet final states can couple only to singlet initial states (and similarly for triplet states), Eq. (16) has the form

$$D_{vv',\alpha\alpha} c_{\alpha a} c_{\alpha b} 2^{-1/2}(M_{cab} + M_{cba})$$

for the diagonal terms, and

$$D_{vv',\alpha\beta}(c_{\alpha a} c_{\beta b} \pm c_{\alpha b} c_{\beta a})(M_{cab} + M_{cba}) \tag{17}$$

for the off-diagonal terms, where the $\pm$ sign denotes the singlet or triplet states, respectively. For $a = b$, the diagonal and singlet off-diagonal terms are the same except for the additional $\sqrt{2}$ factor in the singlet off-diagonal term; the triplet terms are zero. For $a \neq b$, the triplet terms are generally smaller than the singlet terms. The spin symmetry has the effect of reducing the size of the secular determinant since the singlet and triplet configurations form noninteracting subdeterminants.

A common problem with the CI technique is the rapid increase in the number of configurations required with increasing molecule or cluster size. The local nature of the two-hole DOS reflected in the Auger line shape, the relative unimportance of the unfilled bands in insulators, and the spin symmetry, all points made above, assist us greatly in making the problem tractable. In this work the number of configurations never exceeded 50; however, this was in some cases the minimum number necessary for achieving our semiquantitative results.

B. Model problem

To elucidate the role of configuration mixing and hole-hole correlation in Auger line shapes, we examine here and solve analytically a four-orbital problem. As indicated above, the limitation to four orbitals and four or less configurations is a severe restriction, but it does retain the important features and yet is simple enough to offer an intuitive feeling for the correlation effects. Indeed, this is an important aspect the cluster LCAO-MO-CI model has over the Hubbard model which treats infinite systems.[11,12]

The restriction to a four-orbital problem and the desire to have at least two identical subclusters limit us in this model problem to a linear system with triatomic subclusters B-A-B, where we assume that the orbitals on B are hybridized (e.g., sp hybridized). In this respect, B will play the role of the Si and A of the O atoms in SiO_2, as it is generally agreed[19,20] that Si is highly sp^3 hybridized, whereas O undergoes little hybridization. Table I summarizes two cases which are within these limitations: case (a) involving bonding and antibonding orbitals on A and B, case (b) involving nonbonding orbitals on atom A. The secular determinant is most general for case (a); case (b) being the special case when $\alpha_A = \alpha_H$ and $V = \Gamma$.

1. Case (a)

Solution of Eq. (6) for case (a) gives the four MO's

$$\left| i/ii \right\rangle = N_\pm^{1/2}(\varphi_{A_1} + a^\pm \varphi_{H_1} \pm \varphi_{A_2} \pm a^\pm \varphi_{H_2}),$$

$$\left| iii/iv \right\rangle = N_\pm^{1/2}(a^\pm \varphi_{A_1} - \varphi_{H_2} \pm a^\pm \varphi_{A_2} \mp \varphi_{H_2}),$$

(18)

where

$$a^\pm = \frac{A^\pm}{2V} + \left[\left(\frac{A^\pm}{2V}\right)^2 + 1 \right]^{1/2},$$

$$A^\pm = \alpha_H - \alpha_A \pm \Gamma,$$

(19)

$$N^\pm = 1/\{2[1 + (a^\pm)^2]\},$$

and the MO energies are

$$\epsilon_{i/ii} = \epsilon_b^\pm = \alpha_A + \tfrac{1}{2}A^\pm + [(\tfrac{1}{2}A^\pm)^2 + V^2]^{1/2},$$

$$\epsilon_{iii/iv} = \epsilon_a^\pm = \alpha_A + \tfrac{1}{2}A^\pm - [(\tfrac{1}{2}A^\pm)^2 + V^2]^{1/2}.$$

(20)

Appropriate for the case, $\Gamma \ll V$, Eq. (20) has been written to emphasize the existence of two closely spaced bonding orbitals $\epsilon_b^\pm$ and two closely spaced antibonding orbitals $\epsilon_a^\pm$. In an extended system one would obtain a "band" of energies at ϵ_b and one at ϵ_a with bandwidths of the order of Γ and a band gap of the order V.

Assuming in "a" that the bonding orbitals are filled, and the antibonding orbitals empty and

---

TABLE I. Definition of atomic orbitals and Hamiltonian matrix for two model clusters.

(a) Bonding and antibonding bands: B_1-A_1-B_2-A_2-B_3

Atomic orbitals: φ_{A_1}, φ_{A_2}

$$\varphi_{H_1} = (h_{B_1} + h_{B_2})/\sqrt{2}, \quad \varphi_{H_2} = (h'_{B_2} + h_{B_3})/\sqrt{2} \text{ }^a$$

Hamiltonian matrix:

	$\left| \varphi_{A_1} \right\rangle$	$\left| \varphi_{H_1} \right\rangle$	$\left| \varphi_{H_2} \right\rangle$	$\left| \varphi_{A_2} \right\rangle$
$\left\langle \varphi_{A_1} \right|$	α_A	V	0	0
$\left\langle \varphi_{H_1} \right|$	V	α_H	Γ	0
$\left\langle \varphi_{H_2} \right|$	0	Γ	α_H	V
$\left\langle \varphi_{A_2} \right|$	0	0	V	α_A

(b) Nonbonding bands on A: A_1-B_1-A_2-B_2-A_3-B_3-A_4

Atomic orbitals: φ_{A_1}, φ_{A_2}, φ_{A_3}, φ_{A_4}

Hamiltonian matrix:

	$\left| \varphi_{A_1} \right\rangle$	$\left| \varphi_{A_2} \right\rangle$	$\left| \varphi_{A_3} \right\rangle$	$\left| \varphi_{A_4} \right\rangle$
$\left\langle \varphi_{A_1} \right|$	α_A	Γ	0	0
$\left\langle \varphi_{A_2} \right|$	Γ	α_A	Γ	0
$\left\langle \varphi_{A_3} \right|$	0	Γ	α_A	Γ
$\left\langle \varphi_{A_4} \right|$	0	0	Γ	α_A

$^a h_{B_1}$ and h_{B_2} are hybrid lobes which point toward A_1; h'_{B_2} and h_{B_3} point toward A_2.

sufficiently removed from the bonding orbitals $(V > U)$, we have just three possible two-hole configurations: $|i, i\rangle$, $|ii, ii\rangle$, and $|i, ii\rangle$. Further simplification results from symmetry re-

quirements which exclude any mixing of the $|i, ii\rangle$ configuration with the two diagonal configurations. The problem reduces to a 2×2 problem with the secular determinant:

$$
\begin{array}{cc}
& |i, i\rangle \qquad\qquad\qquad\qquad |ii, ii\rangle \\
\begin{array}{c}\langle i, i| \\ \langle ii, ii|\end{array}
& \left[\begin{array}{cc}
2\epsilon_b^+ + \frac{1}{2}U_1(AH)^{++} + \frac{1}{2}U_{12}(AH)^{++} & \frac{1}{2}U_1(AH)^{+-} - \frac{1}{2}U_{12}(AH)^{+-} \\
\frac{1}{2}U_1(AH)^{+-} - \frac{1}{2}U_{12}(AH)^{+-} & 2\epsilon_b^- + \frac{1}{2}U_1(AH)^{--} + \frac{1}{2}U_{12}(AH)^{--}
\end{array}\right]
\end{array}
\tag{21}
$$

where

$$
U_1(AH)^{\pm\pm} = [(\varphi_A + a^\pm \varphi_H)_1^2 \,|\, r_{12}^{-1}\,|\, (\varphi_A + a^\pm \varphi_H)_1^2] = 4N_\pm^2 [u_A + (a^\pm a^\pm)^2 u_H + 2 a^\pm a^\pm u_{A_1 H_1}]
\tag{22}
$$

and

$$
U_{12}(AH)^{\pm\pm} = [(\varphi_A + a^\pm \varphi_H)_1^2 \,|\, r_{12}^{-1}\,|\, (\varphi_A + a^\pm \varphi_H)_2^2] = 4N_\pm^2 [u_{A_1 A_2} + (a^\pm a^\pm)^2 u_{H_1 H_2} + a^\pm a^\pm (u_{A_1 H_1} + u_{A_2 H_1})]
\tag{23}
$$

represent, respectively, the effective interaction between two holes on a single B-A-B cluster and on two different clusters $(B_1 - A_1 - B_2)$ and $(B_2 - A_2 - B_3)$ in the four-atom system. Solutions of the secular equation give the eigenvalues

$$
E^\pm = [4(\epsilon_b^+ + \epsilon_b^-) + U_1(AH)^{++} + U_1(AH)^{--} + U_{12}(AH)^{++} + U_{12}(AH)^{--}]/4
$$
$$
\pm \frac{1}{2}\{[4(\epsilon_b^+ - \epsilon_b^-) + U_1(AH)^{++} - U_1(AH)^{--} + U_{12}(AH)^{++} - U_{12}(AH)^{--}]^2/4 + [U_1(AH)^{+-} - U_{12}(AH)^{+-}]^2\}^{1/2}
\tag{24}
$$

and mixing coefficients

$$
\frac{D_{\pm, i i}}{D_{\pm, i i\, i i}} = \frac{2E^\pm - 4\epsilon_b^+ - [U_1(AH)^{++} + U_{12}(AH)^{++}]}{U_1(AH)^{+-} - U_{12}(AH)^{+-}} .
\tag{25}
$$

The energy of the $|i, ii\rangle$ configuration can be given by the expression

$$
E^0 = \langle 2^{-1/2}(i, ii + ii, i)\,|\,\hat{H}\,|\,2^{-1/2}(i, ii + ii, i)\rangle
$$
$$
= \epsilon_b^+ + \epsilon_b^- + U_1(AH)^+ .
\tag{26}
$$

It has already been assumed that $U \ll V$. To reduce the complexity of Eqs. (24) through (26), we shall assume here that $\Gamma \ll U_1(AH)$. With this assumption, the first term in brackets inside the square root in Eq. (24) is negligible compared to the second. Furthermore, we define the average quantities

$$
\epsilon_b = \tfrac{1}{2}(\epsilon_b^+ + \epsilon_b^-),
$$
$$
U_1(AH) = \tfrac{1}{2}[U_1(AH)^{++} + U_1(AH)^{--}],
$$

etc. Then Eqs. (24)–(26) become

$$
E^- = 2\epsilon_b + U_{12}(AH),
$$
$$
E^0 = 2\epsilon_b + U_1(AH),
\tag{27}
$$
$$
E^+ = 2\epsilon_b + U_1(AH),
$$

and

$$
\frac{D_{\pm, i i}}{D_{\pm, i i\, i i}} = \pm 1 .
\tag{28}
$$

Inserting Eq. (28) into Eqs. (8) and (18) gives

$$
\Psi^- = \sqrt{2}\,N[(\varphi_{A_1} + a\varphi_{H_1})(1)(\varphi_{A_2} + a\varphi_{H_2})(2)
$$
$$
+ (\varphi_{A_2} + a\varphi_{H_2})(1)(\varphi_{A_1} + a\varphi_{H_1})(2)],
\tag{29a}
$$

$$
\overset{0}{\Psi}{}^+ = \sqrt{2}\,N[(\varphi_{A_1} + a\varphi_{H_1})(1)(\varphi_{A_1} + a\varphi_{H_1})(2)
$$
$$
\mp (\varphi_{A_2} + a\varphi_{H_2})(1)(\varphi_{A_2} + a\varphi_{H_2})(2)],
\tag{29b}
$$

where we have defined $Na = \tfrac{1}{2}(N^+a^+ + N^-a^-)$. It is clear that in the states Ψ^+ and Ψ^0 the two holes are localized on the same $B - A - B$ subcluster; in the Ψ^- state, they are localized on different subclusters.

If we insert Eq. (29) into Eq. (16), we can obtain either the A or B Auger intensity. Assuming the initial core hole was on atom A_1, the Auger process picks out the DOS local on atom A_1, or $\varphi_{A_1}\varphi_{A_1}$ terms. If the initial core hole was on atom B_2, it picks out the DOS local on atom B_2, or the terms $\varphi_{H_1}\varphi_{H_1}$, $\varphi_{H_1}\varphi_{H_2}$, and $\varphi_{H_2}\varphi_{H_2}$. The results are

$$
I_{A1}^- = 0,
$$
$$
I_{A1}^0 = 2N^2 |M_{cAA}|^2 = \tfrac{1}{2}I_A ,
\tag{30}
$$
$$
I_{A1}^+ = 2N^2 |M_{cAA}|^2 = \tfrac{1}{2}I_A ,
$$

$$
I_{B2}^- = \tfrac{1}{2}N^2 a^4 |M_{css} - M_{cpp}|^2 ,
$$
$$
I_{B2}^0 = 2N^2 a^4 |M_{csp}|^2 ,
\tag{31}
$$
$$
I_{B2}^+ = \tfrac{1}{2}N^2 a^4 |M_{css} + M_{cpp}|^2 ,
$$

where I_A is the total intensity for the band and M is the atomic Auger matrix element [Eq. (1)] involving the core orbitals on atoms A and B as appropriate. Although we have not specifically introduced s and p orbitals on atom B to this point, we assume here for convenience that the orbitals h_1 and h_2 are sp hybrids, so that $s(p) = (1/\sqrt{2})(h_1 \pm h_2)$.

The intensities in Eqs. (30) and (31) can be contrasted with those obtained from the fold of the one-electron DOS. They are

$$I_{A1}^{ii,ii} = N_-^2 |M_{cAA}|^2 \approx \tfrac{1}{4} I_A ,$$

$$I_{A1}^{i,ii} = 2N_+ N_- |M_{cAA}|^2 \approx \tfrac{1}{2} I_A , \qquad (32)$$

$$I_{A1}^{i,i} = N_+^2 |M_{cAA}|^2 \approx \tfrac{1}{4} I_A ,$$

$$I_{B2}^{ii,ii} = N_+^2 (a^-)^4 |M_{cpp}|^2 ,$$

$$I_{B2}^{i,ii} = 2N_- N_+ (a^+ a^-)^2 |M_{csp}|^2 , \qquad (33)$$

$$I_{B2}^{i,i} = N_-^2 (a^+)^4 |M_{css}|^2$$

at energies

$$E^{ii,ii} = 2\epsilon_b^- + [U_1(AH)^{--} + U_{12}(AH)^{--}]/2 ,$$

$$E^{i,ii} = \epsilon_b^+ + \epsilon_b^- + U_1(AH)^{+-} , \qquad (34)$$

$$E^{i,i} = 2\epsilon_b^+ + [U_1(AH)^{++} + U_{12}(AH)^{++}]/2 .$$

The intensities in Eqs. (30) and (31) are appropriate when $\Gamma \ll U_1(AH) \ll V$; those in Eqs. (32) and (33) when $U_1(AH) \ll \Gamma \ll V$.

A comparison of these results reveals some interesting features. For the case of the initial core hole on atom A, Eqs. (27), (30), and (32) reveal an overall shifting of the same total intensity from the term involving nonlocal final-state holes (one hole on $B_1 - A_1 - B_2$, the other on $B_2 - A_2 - B_3$) to the terms involving local final-state holes (both holes on $B_2 - A_1 - B_2$) as U increases. This is a general result, one which will be examined numerically for larger clusters in SiO$_2$ in Sec. III. The situation is significantly different when the initial hole is on atom B. First, as U_1 increases, the total intensity changes due to increasing interference effects between the M_{css} and M_{cpp} contributions in the large U case. Second, even when $U \gg \Gamma$, the intensity from the term involving nonlocal final-states holes I_{B2}^- does not necessarily go to zero. In fact, it may be larger than I_{B2}^+; this depends on the signs of M_{css} and M_{cpp}. In summary, we can say for $U \gg \Gamma$, the Auger process on the A_1 atom samples the DOS local to the smaller $B_1 - A_1 - B_2$ subcluster; the Auger process on the B_2 atom samples the DOS on the larger $B_1 - A_1 - B_2 - A_2 - B_3$ cluster but with significant hole-hole "correlation" effects.

An examination of several cases reveals that quite generally $I_{B_2}^+$ is less than $I_{B_2}^-$, i.e., M_{cpp} and M_{css} have opposite signs. For the case at hand, the sp_z hybrid and a 1s initial core hole on B_2, we have

$$(M_{css} \pm M_{cpp})^2 = \sum_l \langle 1s\, kl | r_{12}^{-1} | (ss \pm p_z p_z) \rangle^2$$

$$= [R^0(ssss) \pm \tfrac{1}{2} R^0(sspp)]^2 \qquad (35)$$

$$+ \tfrac{4}{45} [R^2(sdpp)]^2 ,$$

where R is the radial integral:

$$R^k(sll'l') = \int_0^\infty \int_0^\infty R_{1s} R_{kl} \left| \frac{r_<^k}{r_>^{k+1}} \right| R_{n_1'} R_{n_1'} r_1^2 r_2^2 dr_1 dr_2 . \qquad (36)$$

For atoms in the first rows of the periodic table, $R^0(ssss)$ is positive and $R^0(sspp)$ is negative.[21] For the $K - LL$ transitions in atoms, Asaad[22] has found that CI effects decrease the KL_1L_1 intensity and increase the $KL_{23}L_{23}$ intensity. McGuire[23] determined that CI effects decrease the $L_{23}M_1M_1$ intensity in Cu and Zn and increase the $L_{23}M_{23}M_{23}$ intensity.

2. Case (b)

Case (b) involves four nonbonding orbitals on four A atoms as indicated in Table I. It is a special case of (a), namely, when $\epsilon_A = \epsilon_H$, and $V = \Gamma$; hence the molecular orbitals and energies are still given by Eqs. (18)–(20). More specifically, these equations give

$$|i/ii\rangle = N_\pm^{1/2} (\varphi_{A_1} + a^\pm \varphi_{A_2} \pm \varphi_{A_3} \pm a^\pm \varphi_{A_4}) , \qquad (37)$$

$$|iii/iv\rangle = N_\pm^{1/2} (a^\pm \varphi_{A_1} - \varphi_{A_2} \pm a^\pm \varphi_{A_3} \mp \varphi_{A_4}) ,$$

$$a^\pm = \pm \tfrac{1}{2} + (5/4)^{1/2} , \qquad (38)$$

and

$$\epsilon_{i/ii} = \alpha_A + \tfrac{1}{2} \Gamma(\sqrt{5} \pm 1) , \qquad (39)$$

$$\epsilon_{iii/iv} = \alpha_A - \tfrac{1}{2} \Gamma(\sqrt{5} \mp 1) .$$

Assuming that all the nonbonding orbitals are filled, we have ten possible two-hole configurations. In the event $U \ll \Gamma$, a negligible CI mixing occurs, and the two electron energies and Auger intensities are given simply as

$$E_{\alpha\beta} = \epsilon_\alpha + \epsilon_\beta \quad (\alpha, \beta = i \text{ to } iv) , \qquad (40)$$

$$I_{\alpha\beta} = N_\pm N_\mp [(a^\pm a^\mp)^2, (a^\pm)^2, \text{ or } 1] |M_{cAA}|^2 \qquad (41)$$

where the initial core hole is assumed to be on atom A_2 and the proper choice in Eq. (41) is obvious. The total sum $\sum_{\alpha\beta} I_{\alpha\beta}$ equals $|M_{cAA}|^2$.

In the event $U \approx \Gamma$, the analytical solution of a

10×10 secular determinant is formable even though the problem is simplified somewhat by symmetry. Much more instructive at this point is to examine the problem when $U \gg \Gamma$. This can

be examined more simply by omitting the construction of the MO's and constructing the two-hole configurations directly in terms of the atomic orbitals φ_A. The Hamiltonian matrix becomes

$$
\begin{array}{c}
\\
\langle 11| \\
\langle 22| \\
\langle 33| \\
\langle 44| \\
\langle 12| \\
\langle 23| \\
\langle 34| \\
\langle 13| \\
\langle 24| \\
\langle 14|
\end{array}
\begin{array}{c}
|11\rangle \quad |22\rangle \quad |33\rangle \quad |44\rangle \quad |12\rangle \quad |23\rangle \quad |34\rangle \quad |13\rangle \quad |24\rangle \quad |14\rangle \\
\left[
\begin{array}{cccccccccc}
u_1 & & & & & & & & & \\
0 & u_1 & & & & & & & & \\
0 & 0 & u_1 & & & & & & & \\
0 & 0 & 0 & u_1 & & & & & & \\
\sqrt{2}\,\Gamma & \sqrt{2}\,\Gamma & 0 & 0 & u_{12} & & & & & \\
0 & \sqrt{2}\,\Gamma & \sqrt{2}\,\Gamma & 0 & 0 & u_{12} & & & & \\
0 & 0 & \sqrt{2}\,\Gamma & \sqrt{2}\,\Gamma & 0 & 0 & u_{12} & & & \\
0 & 0 & 0 & 0 & \Gamma & \Gamma & 0 & u_{13} & & \\
0 & 0 & 0 & 0 & 0 & \Gamma & \Gamma & 0 & u_{13} & \\
0 & 0 & 0 & 0 & 0 & 0 & 0 & \Gamma & \Gamma & u_{14}
\end{array}
\right] ,
\end{array}
$$

$$(42)$$

where the $|ij\rangle$ now refer to atomic configurations $\varphi_{A_i}\varphi_{A_j}$. In Eq. (42) we have omitted the $2\,\alpha_A$ term from each of the diagonal elements and utilized the ZDO approximation as usual. The symbols u_{ij} refer to Coulomb matrix elements on the same center and between the 1st-, 2nd-, and 3rd-nearest neighbors, respectively.

The diagonalization of Eq. (42) produces the same eigenvalues and eigenvectors as the diagonalization of the Hamiltonian matrix constructed from the ten MO configurations. In general, the Hamilton matrix is more difficult to diagonalize in the atomic basis because symmetry considerations do not simplify the problem as in the MO basis. Nevertheless, if $u_i \gg \Gamma$ or more critically $(u_i - u_{ij})_{i \neq j} \gg \Gamma$, this matrix is essentially already diagonal and the solution becomes trivial. The Auger process samples the DOS local on atom A_2; the entire Auger intensity $|M_{cAA}|^2$ coalesces to one narrow peak at energy $2\alpha_A + u_1$.

The case (b) as described is appropriate for the nonbonding orbitals on O in the SiO_2 system. In Sec. III we will examine the coalescence to a single peak as u_i increases relative to Γ, and also examine the effects of cluster size and the effects of the two-center u_{ij}.

III. RESULTS AND DISCUSSION

We have performed various MO calculations on several different clusters, always with a minimal basis set and at times with a partial minimal set. The valence one-electron DOS in SiO_2 fall roughly into three major groups: the "O_{2s}" bond-

ing states grouped about 20 eV below the edge (the $4a_1$ and $3t_2$ orbitals of the tetrahedral SiO_4 cluster), the "O_{2p}" (b) bonding states grouped about 6 eV below the edge (the $5a_1$ and $4t_2$ orbitals), and the O_{2p} (nb) nonbonding states located just below the edge (the $1e$, $5t_2$, and $1t_1$ orbitals). We have examined the $O_{2p}(b)$ and the $O_{2p}(nb)$ states on the Si_4O_3 and Si_8O_7 clusters with O as central atom, the O_{2s}, $O_{2p}(b)$, and $O_{2p}(nb)$ states on a Si_5O_4 cluster with Si as central atom, and the $O_{2p}(nb)$ density of states on O_3, O_7, and O_{16} clusters. A beta crystobalite crystal structure (Si–O–Si angle equal 180°) is used throughout with Si–O bond length equal 1.5 Å.[24] The initial core hole is placed in a central Si_2O subcluster, nearest-neighbor subclusters are placed in the proper crystal structure building outwardly to assemble the complete cluster.

The matrix elements in Eq. (6) were treated as parameters determined so that the resultant one-electron MO energies and orbital populations are similar to our previously determined SiO_2 DOS.[1] An optimal set of matrix element parameters, determined from the above-indicated calculations, is reported in Table II and compared with corresponding tight-binding parameters as recently reported.[14,25] In general, the agreement is quite satisfactory considering our calculations involve a minimal basis set on rather small clusters. The $V(O_{2s}, O_{2s})$ and $V(O_{2p}, O_{2p})$ elements include both direct and indirect "hopping" or interaction terms, i.e., hopping terms which involve the Si atom are included. In fact,

TABLE II. Summary of matrix elements (tight-binding parameters) obtained in this work and comparison with other reported results.

Matrix element	This work (eV)	Tight-binding calc. (eV)	
		Chadi et al.[a]	Nucho et al.[b]
$\alpha(\text{Si}_h)$	-3 $(-4)^c$	-4.6 [d,e]	-7.9 [d]
$\alpha(\text{O}_{2s})$	24	19.1 [d]	
$\alpha(\text{O}_{2p})$	6 $(5,8)^c$	6.3 [d]	6.0 [d]
$V(\text{O}_{2s},\text{O}_{2s})$	0	0.15	
$V(\text{O}_{2p},\text{O}_{2p})$	1	0.45	
$V(\text{Si}_h,\text{Si}_h)$	2^f	1.6 [g]	
$V(\text{Si}_h,\text{O}_{2s})$	5	6.2 [g]	
$V(\text{Si}_h,\text{O}_{2p})$	6^f	5.4 [g]	$5,2$ [h]
$u(\text{O}_{2s})$	15^i		
$u(\text{O}_{2p})$	15^i		
$u(\text{Si}_h)$	11 [i,j]		

[a]Reference 14.

[b]Reference 25.

[c]Values in parentheses were used for the Si_4O_5 cluster where $\alpha(\text{O}_{2p}(b))$ and $\alpha(\text{O}_{2p}(nb))$ were allowed to be different, i.e., 5 and 8, respectively.

[d]4.5 eV added to literature values to change zero-point energy from the top of the valence band to the Fermi level (Ref. 1).

[e]$\alpha(\text{Si}_h) = [\alpha(\text{Si}_{3s}) + 3\alpha(\text{Si}_{3p})]/4$ for sp^3 hybrid (Ref. 40). Values of $\alpha(\text{Si}_{3s})$ and $\alpha(\text{Si}_{3p})$ from Ref. 14.

[f]In the Si_4O_3 cluster calculations, a linear combination of the sp^3 hybrids h_i were utilized, i.e., $H = (1/\sqrt{2})(h_1 \pm h_2)$. Thus $V(\text{Si}_H,\text{Si}_H) = \frac{1}{2}V(\text{Si}_h,\text{Si}_h) = 1$ and $V(\text{Si}_H,\text{O}_{2p}) = \sqrt{2}V(\text{Si}_h,\text{O}_{2p}) = 9$.

[g]$V(\text{Si}_h,\text{Si}_h) = \frac{1}{4}[\alpha(\text{Si}_{3s}) - \alpha(\text{Si}_{3p})]$ (Ref. 40). $V(\text{Si}_h,\text{O}_{2s/p}) = \frac{1}{2}[V(\text{Si}_{3s},\text{O}_{2s/p_\sigma}) + V(\text{Si}_{3p_\sigma},\text{O}_{2s/p_\sigma})]$, where by symmetry $V(\text{Si}_{3p_\Pi},\text{O}_{2s/p_\sigma}) = 0$.

[h]Two different sets of parameters were reported, the values depending upon the region of the DOS fitted (Ref. 25).

[i]u was treated throughout as a parameter in the calculations to gradually turn on the effects of correlation. However, our best estimates are given here as determined from Mann's (Ref. 18) integral tables and estimates of the correlation or static relaxation contributions (Ref. 1).

[j]$u(\text{Si}_H) = \frac{1}{2}[u(\text{Si}_{h_1}) + u(\text{Si}_{h_1},\text{Si}_{h_2})] = 7$.

the presence of the Si atoms in the $\text{O}_{16}\text{O}_{2p}(nb)$ calculation is exhibited only through these terms. Only hopping matrix elements involving two oxygen atoms connected through a common Si atom are assumed to be significant. All others are set to zero. Likewise, only nearest-neighbor bonded Si–O elements are included. Appropriate values for the matrix elements involving the Si sp^3 hybrid orbital h_i are obtained as indicated in the Table.

The values of u tabulated in Table II are obtained from the integrals of Mann[18]; however, a static relation term r has been subtracted off. These have been estimated previously[1] to be 6 eV for O $2s$ and $2p$ orbitals, and 2(1) eV for Si $3s(3p)$ orbitals. Huang[15] has given the formula for obtaining the $u(\text{Si}_h)$ result from the $u(\text{Si}_{3s/p})$ elements. $u(\text{O}_{2p})$ has also been determined empirically by Oleari et al.[26] who obtained a value of 14.5 eV. The empirical result is said to include correlation effects (i.e., static relaxation effects).

A. O KLL line shape

Results for the O KLL Auger line shape obtained from the linear Si_4O_3 cluster involving the O_{2p} bonding and nonbonding orbitals are given in Fig. 2. These results were obtained from a 12-orbital system; namely 3 $\text{Si}_H \equiv (1/\sqrt{2})(h_1 - h_2)$ orbitals, 3 $\text{O}_{2p}(b)$, and 6 $\text{O}_{2p}(nb)$ atomic orbitals. In this system, symmetry allows mixing only between the $\text{O}_{2p\sigma}$ and Si_H orbitals giving MO's belonging to the O_{2p} bonding and antibonding groups; however, the antibonding MO's are unoccupied. Thus the $b - b$, $b - nb$, and $nb - nb$ two-hole configurations are mixed in separate CI calculations. The results show clearly the effects of increasing correlation (increasing u), most notably in the coalescence of most of the Auger intensity into a rather narrow band around 502 eV. Clearly, this band corresponds to both holes localized on to the same Si–O–Si cluster. The $\text{O}_{2p}(nb)$ lines are shifted down by ~15 eV as they are localized

$u_0(u_{Si}) = 0(0)$	5(2) eV	15(7) eV

AUGER ENERGY (eV)

520 ———————— 100

518
            200
516 ═⇒ 35   34
     ═⇒ 38   3
514 ———— 100   55
     ⇒ 5   10
512 ≡14 ═38   28   133 4
     ═ 26
     12   .6
510   ═⇒32 5   177   .6
                 ⇐   78
508 ═16   .4
         31

506

504

502   20   133
                 ════   120
                 ———— 52   254
500
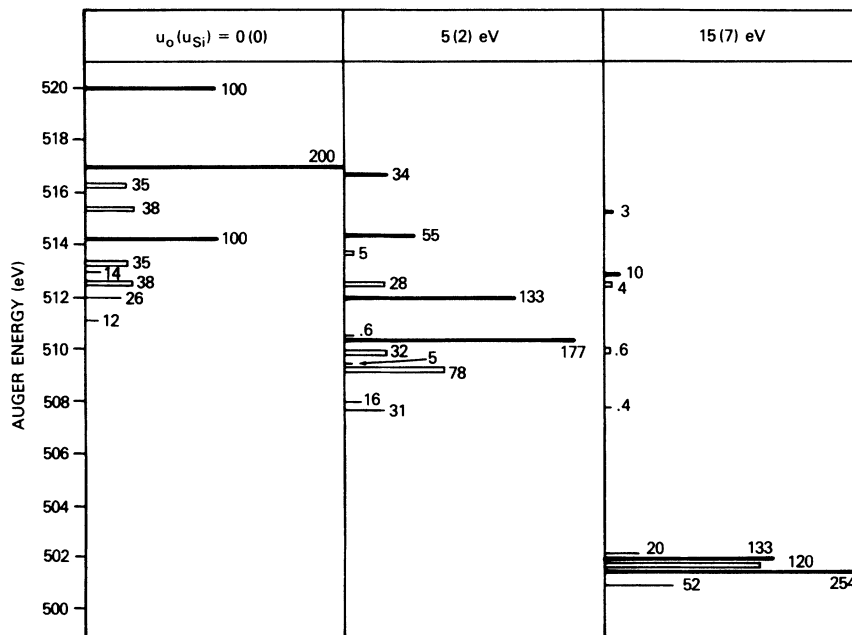
FIG. 2. Auger energies and relative intensities of the eigenvalues arising from an LCAO-MO-CI calculation on the Si_4O_3 cluster for various values of u_O and u_{Si}. Contributions from the $O_{2p}(b)$-$O_{2p}(b)$, $O_{2p}(nb)$-$O_{2p}(b)$, and $O_{2p}(nb)$-$O_{2p}(nb)$ bands are indicated by the light solid, open, and heavy solid lines, respectively. Contributions involving the O_{2s} band are ignored here. Numbers indicate the intensity in arbitrary units.

on a single O atom; the $O_{2p}(b)$ lines just 11 eV (the approximate hole-hole repulsion on the Si–O–Si cluster in the $O_{2p}(b)$ MO). Note the appearance of residual nonlocal contributions shifted down by just 4 eV (the approximate hole-hole repulsion when the holes are on different Si–O–Si clusters). Ignoring these residual contributions, the Auger O_{2p} line shape narrows from ~9 to ~2 eV, giving essentially an atomic O Auger spectrum.

Since the greatest share of the 502-eV peak of the O KLL Auger line shape comes from the (nb, nb) transitions, we can for the moment ignore all other contributions. This allows for a study of much larger clusters and hence also a study of cluster-size effects. Results of calculations on the O_{16} clusters are given in Fig. 3, where just Auger (nb, nb) contributions are examined. The one-electron DOS and the two-hole DOS resulting from a CI involving 37 configurations are shown. Similar trends are revealed, namely, a coalescence to a local peak shifted down in energy by an amount u_1 and several residual nonlocal peaks.

Figure 4 summarizes results of calculations on O_3, O_7, and O_{16} clusters when all two-center hole-hole repulsion integrals are set to zero. Plotted in Fig. 4 is the intensity in the residual nonlocal peaks relative to the total intensity (always normalized to 100 in these calculations) and the dif-

ference in energy between the centroids of the local and nonlocal contributions versus u/Γ. u/Γ is the one-center hole-hole repulsion on the oxygen atom divided by the one-electron $O_{2p}(nb)$ bandwidth. The results plotted depend only on u/Γ and not on u and Γ individually, and no other parameters are present in these calculations. As one might expect, the results from the different cluster sizes converge with increasing u/Γ; for large u/Γ the Auger line shape is increasingly dominated by the local peak where both holes are on a single O atom. In the physical range of interest, $u/\Gamma \approx 2$–4, it would appear that the O_7 cluster size is already sufficient.

Also plotted in Fig. 4 are results of a calculation on the O_{16} cluster when the two-center integrals u_{ij} are included as estimated from the Mataga-Nishimoto approximation, Eq. (13). In these calculations, the u_{ij} increase with increasing u/Γ. The inclusion of the u_{ij} appears to decrease the effective size of the one-center u_i, as one might expect. However, it should be pointed out the the full effects of u_{ij} cannot be completely compensated for by decreasing the effective u_i. The shift down in absolute energy of the total Auger line shape increases when the u_{ij} are included, but a decrease in u_i would decrease this shift.

The difference peak at 511 eV in the O KLL Auger line shape (Fig. 1) is estimated to have

ONE-ELECTRON LOCAL DOS	$u_1 = 0$ eV $u_{12} = 0$	5 eV 2.7	11 eV 3.8	15 eV 4.1	PEAK NO.
62.0	38.5				
9.0	11.2	16.9			
13.0	16.9	12.6	4.5	3.9	1
16.0	19.8	18.4	8.4	3.8	2
	13.6	31.5	10.1	3.9	3
		20.6	23.3	8.4	
			53.7	80.0	4
					5
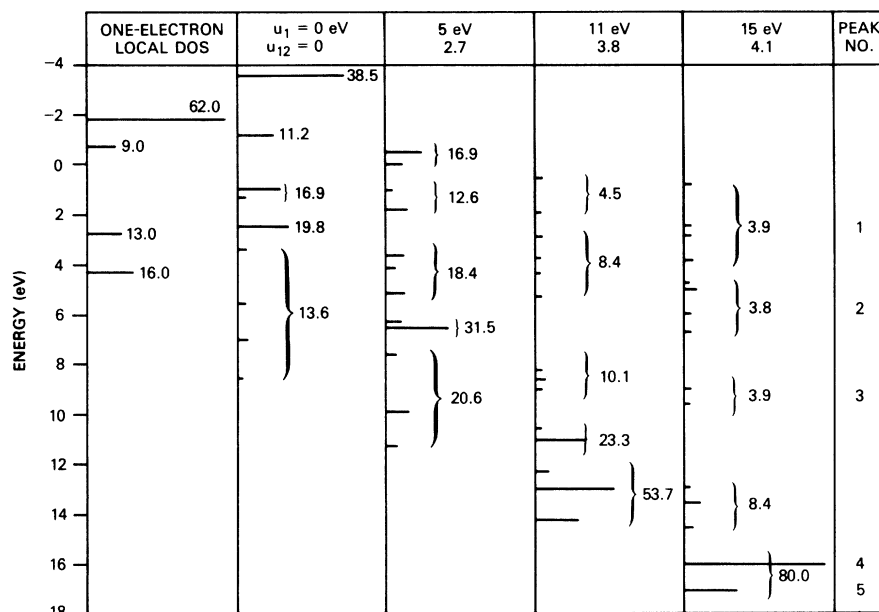
FIG. 3. Column one contains the one-electron $O_{2p}(nb)$ local density of states on the central O atom arising from an LCAO-MO calculation on an O_{16} cluster. Columns two through four contain the relative $O_{2p}(nb)$-$O_{2p}(nb)$ Auger energies and intensities of the eigenvalues arising from a CI calculation on the O_{16} cluster for various values of one- and two-center hole-hole repulsion integrals u_1 and u_{12}. The total intensity has been normalized to 100. The local DOS energies are equal to 16 eV minus the energies indicated; the Auger energies are equal to 517 eV minus the energies indicated. The peak numbers refer to Table III. The $O_{2p}(nb)$ bandwidth as exhibited in column one is ~6 eV.

about 20% of the intensity of the theoretical Auger peak at 504 eV (the shake satellite intensity is not included in the 504-eV peak here). If this difference peak is attributed to the nonlocal Auger contributions, the 7-eV experimental separation between the local and nonlocal peaks provides an estimate of 2.5 for u/Γ (from Fig. 4, using the O_{16} nonzero u_{ij} plot). Furthermore, the 17% experimental intensity ratio between the difference peak at 511 eV and the total (504-eV peak plus 511-eV peak) indicates a u/Γ value of 2.5 (also from Fig. 4, nonzero u_{ij} plot). That the two estimates are in agreement is most gratifying and supports rather strongly the assumption that the 511-eV shoulder is indeed due to the nonlocal contributions. Note that the O_{16} results obtained for zero u_{ij} would give conflicting values for u/Γ.

The value of 2.5 for u/Γ is a reasonable one. The best estimate of $u(O_{2p})$, as given in Table II, is 15 eV. This indicates a value of 6 eV for Γ. Band calculations[14,19,20,25,27,28] have given results varying from 1 to 5 eV for the bandwidth of the O_{2p} nonbonding band with perhaps the most reliable theoretical result around 5 eV.[20,27] X-ray-emission data and UPS data in SiO_2 suggest a value around 4 eV (Refs. 27, 29-31).

We can suggest two possible causes for our 1-2-eV overestimate of Γ. The determination

of a bandwidth from a relatively small cluster calculation is nebulous at best. The O_{16}-cluster calculations provide a spectrum of eigenvalues the breadth of which provides our estimate of the bandwidth. This is probably the best procedure since in band calculations, Γ represents the full width of the DOS. Secondly, our results depend on the values of the u_{ij}. This is indicated in Fig. 4 for the two-O_{16}-cluster calculations, one including the u_{ij}, the other not. If the Mataga-Nishimoto approximation underestimates the u_{ij} (we will present some evidence later that this may be the case), our estimate of Γ will be too large. Evidently as u_{ij} increases, both the relative-intensity and energy-difference curves move to higher u/Γ and hence indicate a smaller Γ.

It is of interest from an intuitive point of view to note the relative location of the two holes formed in the Auger process. Table III contains the probabilities P_{ij} for hole occupancy on the ith and jth O atoms in the $O_{2p}(nb)$ band of SiO_2. For simplicity, these results come from an O_7 cluster calculation rather than the O_{16} cluster. The two "local" Auger peaks, peaks 4 and 5 (peak numbers are indicated in Fig. 3), clearly correspond to a high hole occupancy on the same O atom as anticipated for large u. The three "nonlocal" peaks in order of decreasing energy
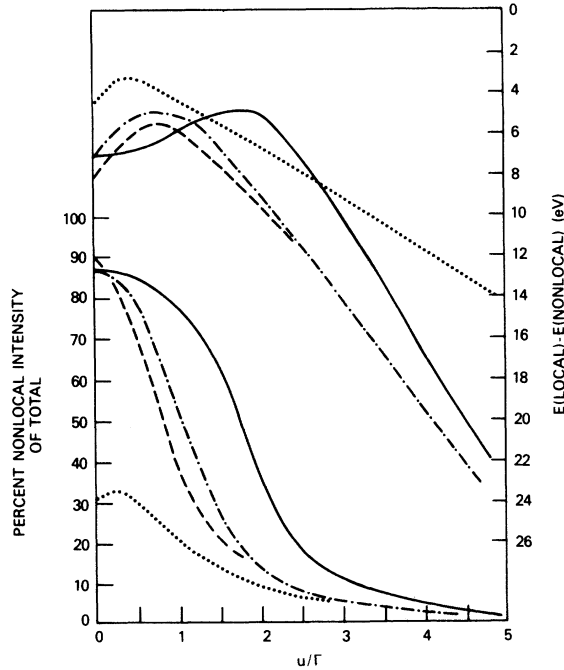
FIG. 4. Comparison of results for the $O_{2p}(nb) - O_{2p}(nb)$ Auger line shape. On the lower left is plotted the percent nonlocal intensity of the total Auger intensity versus u/Γ. On the upper right is plotted the difference in energy between the centroids of the local and nonlocal Auger contributions versus u/Γ. u is the one-center hole-hole repulsion energy parameter; Γ is the $O_{2p}(nb)$ bandwidth as determined from the spread of the one-electron DOS of the corresponding n cluster. Results are shown for clusters containing three atoms (dotted line), seven atoms (dashed line), 16 atoms with $u_{ij} = 0$ (dot-dashed line), and 16 atoms with $u_{ij} \neq 0$ (solid line).

can be described as follows: At peak (3) the hole occupancy is predominantly on 2nd- and 3rd-near neighbors with a significant probability (~ 0.11) for both holes on the same center; at peaks (2) and (1), the hole occupancy is predominantly on nearest neighbors but with significant probability for occupancy on 2nd- and 3rd-near neighbors also. The Auger intensity is directly proportional to P_{11} (both holes occupying the atom with the initial core hole). It would appear the Auger energy is primarily determined by the total of the one-center occupancy terms as the "nonlocal" peaks are ordered in energy accordingly. The relative occupancy of nearest neighbors and 2nd- and 3rd-near neighbors is unimportant in determining energy apparently because the $1/R$ behavior reduces u_{12} already to ~ 4 eV (when u_1 is 15 eV), and the higher terms (e.g., u_{13}, u_{25}, etc.) are only slightly smaller.

B. Si L_{23} VV line shape

Results for the Si $L_{23}VV$ Auger line shape obtained from the tetrahedral Si_5O_4 cluster is given in Fig. 5. These results were obtained from a 16 orbital system, namely, four Si_h orbitals on the central Si, one Si_h orbital on each of the edge Si atoms and an O $2s$ and $2p_z$ orbital on each of the four O atoms. The O $2p_x$ and $2p_y$ nonbonding orbitals were ignored in this calculation. The resultant one-electron MO's are named in the T_d point group $4a_1(3s)$, $3t_2(3p)$, $5a_1(3s)$, and $4t_2(3p)$, where the dominant contribution of the Si atom in each MO is indicated in parentheses. Although the MO calculations are performed with sp^3 hybrids (h_i) on the Si atoms, solution of the secular equation automatically provides for the proper linear combination of these hybrids to give back either an s or p orbital as dictated by symmetry. Upon performing the CI with increasing u_i, the orbitals rehybridize.

The number of two-hole configurations necessary for an appropriate hole-hole correlation treatment can again be kept to a minimum. The energy spacing between the $4a_1$, $3t_2$ orbitals (the O_{2s} band) and the $5a_1$, $4t_2$ orbitals [the $O_{2p}(b)$ band] is large compared to the effective hole-hole repulsion in the Si_5O_4 cluster, so the configurations from the $O_{2s} - O_{2s}$, $O_{2s} - O_{2p}$, and $O_{2p} - O_{2p}$ bands can again be mixed in separate CI calculations. Group theoretic arguments can be used to simplify the problem still further. Thus in the diagonal cases (either $O_{2s} - O_{2s}$ or $O_{2p} - O_{2p}$) we have the configurations leading to the terms

$$a_1^2 - {}^1A_1,$$

$$a_1 t_2 - {}^1T_2, {}^3T_2,$$ (43)

$$t_2^2 - {}^1A_1, {}^3T_1, {}^1E, {}^1T_2,$$

and in the nondiagonal case $O_{2s} - O_{2p}$, the terms

$$a_1 a_1' - {}^1A_1, {}^3A_1,$$

$$a_1 t_2' - {}^1T_2, {}^3T_2,$$ (44)

$$a_1' t_2 - {}^1T_2, {}^3T_2,$$

$$t_2 t_2' - {}^1A_1, {}^3A_1, {}^1T_2, {}^3T_2, {}^1E, {}^3E, {}^1T_1, {}^3T_1.$$

Since only terms of the same symmetry and multiplicity mix, the complete CI is easily tractable (e.g., in the diagonal cases, mixing occurs only between the two ${}^1A$ terms and only between the two ${}^1T_2$ terms).

Expressions for determing the Auger intensity are given in Table IV. These expression involve the CI mixing coefficients D obtained from Eq. (9),

TABLE III. Probabilities P_{ij} for hole occupancy on the ith and jth O atoms in the 2p nonbonding band of an O_7 cluster in SiO_2.

Peak[a]	u	Energy of state in band	Same center P_{11}[b]	Same center ΣP_{ii} $i \neq 1$	Nearest neighbor ΣP_{1i} $i \neq 1$	Nearest neighbor $\Sigma {}^c P_{ij}$ $i \neq j \neq 1$	2nd and 3rd neighbors, etc. $\Sigma {}^d P_{ij}$ $i \neq j \neq 1$
	0	−3.29	0.475	0.016	0.429	0.032	0.048
1	5	0.20	0.275	0.018	0.528	0.092	0.104
	8	1.31	0.151	0.000	0.563	0.138	0.148
	15	2.54	0.043	0.000	0.556	0.177	0.224
	0	−2.00	0.000	0.435	0.000	0.390	0.176
2	5	2.06	0.019	0.502	0.013	0.460	0.006
	8	3.74	0.024	0.322	0.037	0.577	0.039
	15	5.60	0.003	0.074	0.024	0.678	0.222
	0	2.00	0.429	0.071	0.143	0.143	0.214
3	5	5.51	0.399	0.007	0.009	0.044	0.581
	8	6.63	0.216	0.020	0.034	0.001	0.730
	15	8.16	0.072	0.043	0.281	0.056	0.547
	0	4.00	0.000	0.167	0.000	0.333	0.500
4	5	7.01	0.139	0.342	0.468	0.274	0.197
	8	9.19	0.357	0.432	0.042	0.143	0.027
	15	15.55	0.447	0.505	0.011	0.037	0.001
	0	7.29	0.096	0.079	0.429	0.158	0.237
5	5	10.38	0.166	0.147	0.401	0.170	0.116
	8	11.93	0.251	0.226	0.324	0.142	0.057
	15	16.87	0.435	0.379	0.127	0.052	0.007

[a] Peak numbers correspond to those in Fig. 3.
[b] Atom 1 is the atom with the initial core hole.
[c] Only P_{ij} terms in which i and j are nearest neighbors are included.
[d] Only P_{ij} terms in which i and j are not nearest neighbors are included.
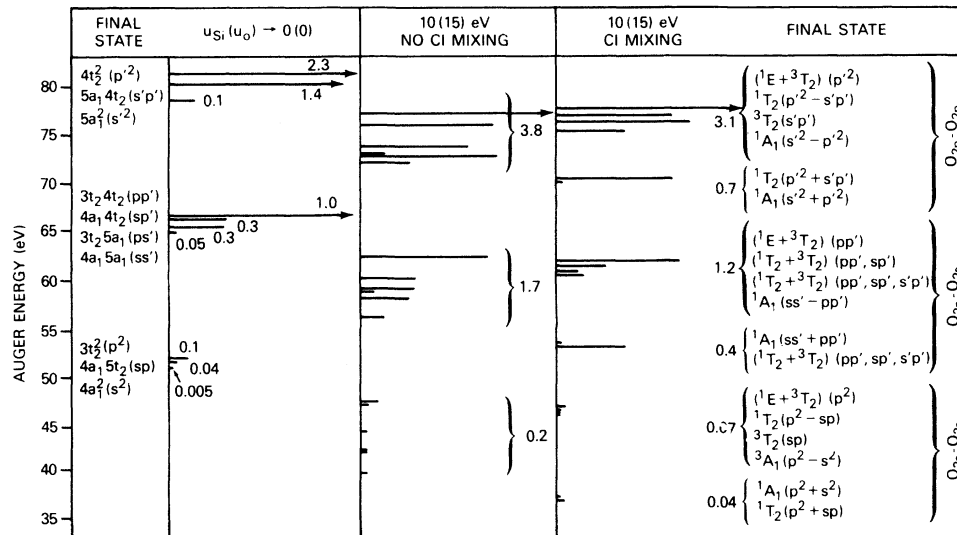
FIG. 5. Comparison of results for the Si $L_{23}VV$ Auger line shape. In column one are the Auger energies and relative intensities resulting from the fold of the one-electron DOS local to the central Si atom as determined from an LCAO-MO calculation on an Si_5O_4 cluster. The position of the final-state holes is indicated at the far left in terms of the MO's as named in tetrahedral symmetry. The symbols (s, p) in parentheses indicate the dominant central Si atom contribution. In column two, hole-hole repulsion is included without CI mixing for $u_{si} = 10$ and $u_0 = 15$ eV. The third column gives results with CI mixing. The terms ${}^{2S+1}(A, E$ or $T)$ are given as determined by group theory in T_d symmetry; the dominant configuration mixing given in parentheses after the term symbol. Numbers given indicate intensities in arbitrary units.

TABLE IV. The Auger transition rates after CI mixing of the terms coming from the tetrahedral Si_5O_4 cluster.

Molecular term [a]		Transition rate
	$^1A_1$ (2)	$[D(a_1^2, {}^1A_1)c_s^2(a_1)M_{css}(^1S)$ $+ D(t_2^2, {}^1A_1)c_p^2(t_2)M_{cpp}(^1S)]^2$
$O_{2s}-O_{2s}$	$^1T_2$ (2)	$[D(a_1t_2, {}^1T_2)c_s(a_1)c_p(t_2)M_{csp}(^1P)$ $+ D(t_2^2, {}^1T_2)c_p^2(t_2)(0.6)M_{cpp}(^1D)]^2$
or		
$O_{2p}-O_{2p}$	$^3T_2$	$[c_s(a_1)c_p(a_1)M_{csp}(^3P)]^2$
terms	$^3T_1$	$[c_p^2(t_1)M_{cpp}(^3P)]^2$
	^1E	$[c_p^2(t_2)(0.4)M_{cpp}(^1D)]^2$
	$^{1/3}A_1$ (4)	$[D(a_1a_1', {}^{1/3}A_1)c_s(a_1)c_s(a')M_{css}({}^{1/3}S)$ $+ D(t_2t_2', {}^{1/3}A_1)c_p(t_2)c_p(t_2')M_{cpp}({}^{1/3}S)]^2$
	$^{1/3}T_2$ (6)	$[D(a_1t_2', {}^{1/3}T_2)c_s(a_1)c_p(t_2')M_{csp}({}^{1/3}P)$
$O_{2s}-O_{2p}$		$+ D(a_1't_2, {}^{1/3}T_2)c_s(a_1')c_p(t_2)M_{csp}({}^{1/3}P)$
terms		$+ D(t_2't_2, {}^{1/3}T_2)c_p(t_2)c_p(t_2')(0.6)M_{cpp}({}^{1/3}D)]^2$
	$^{1/3}E$	$[c_p(t_2)c_p(t_2')(0.4)M_{cpp}({}^{1/3}D)]^2$
	$^{1/3}T_1$	$[c_p(t_2)c_p(t_2')M_{cpp}({}^{1/3}P)]^2$

[a] Number in parentheses indicates number of states having this symmetry.

the atomic orbital coefficients c obtained from solution of Eq. (6), and the atomic Auger matrix elements in LS coupling $M_{cll'}(^{2S+1}L)$. Expressions for evaluating $M_{cll'}(^{2S+1}L)$ have been reported by McGuire[23] and others.[22,32,33] The $M_{cpp}(^3S)$, $M_{cpp}(^3D)$, $M_{cpp}(^1P)$, and $M_{css}(^3S)$ matrix elements are equal to zero in this work, as shown in Eq. (17) and Sec. II A. The five ^1D states in spherical symmetry split into the ^1E and $^1T_2$ terms in tetrahedral symmetry. The ^1D intensity splits up equally, one fifth into each of the states regardless of symmetry.[34] As determined by McGuire, $M_{css}(^1S)$ and $M_{cpp}(^1S)$ are of different sign so that the $a_1^2 + t_2^2$ has a smaller intensity than the $a_1^2 - t_2^2$ state.

Figure 5 compares results with no hole-hole repulsion effects, with hole-hole repulsion effects but without CI mixing, and with complete CI mixing. The turn on of hole-hole repulsion without CI mixing causes additional lines from multiplet splitting. The turn on of CI mixing then coalesce these terms into local and nonlocal contributions for each band ($O_{2s} - O_{2s}$, $O_{2s} - O_{2p}$, and $O_{2p} - O_{2p}$). In this instance, the local contributions correspond to both holes localized on an Si_2O subcluster with $U_{eff} \approx 11$ eV, and the nonlocal contributions to the holes localized on different Si_2O subclusters with $U_{eff} \approx 4$ eV. Because the initial core hole was on the central Si atom with a local Si population in all four Si_2O subclusters, the Auger intensity now does not coalesce into just the local

peak as in the O KLL case, but a major part of the Auger intensity remains in the nonlocal contributions.

Nevertheless, the effects of CI mixing appear to be evident in the Si $L_{23}VV$ line shape. The local contribution of the $O_{2s}O_{2p}$ band at ~ 54 eV now matches up more with the 50 eV peak in the experimental Auger line shape of Fig. 1. The 0.4 relative intensity of this peak also is of the proper magnitude to account for the intensity under the experimental peak since the theoretical peak was way too small in the earlier work. The shoulder at 68 eV in the experimental line shape we have previously suggested may be due to a shake satellite. It now appears it could be due to the local contribution of the $O_{2p}O_{2p}$ band at ~ 70 eV with a relative intensity of 0.7. The intensity of 0.7, somewhat less than the nearby 1.2 intensity of the contributions at 63 eV, seems qualitatively correct if it is to account for the 68-eV shoulder. The small local contribution of the $O_{2s}O_{2s}$ band at 37 eV falls under the Si $L_1L_{23}V$ peak which we examined earlier.[1]

It appears that the local contribution is sufficiently removed in energy from the nonlocal contributions that they tend to fall under different experimental peaks and thus final-state correlation effects are visible in the Si $L_{23}VV$ Auger line shape. Although the energy alignment (both absolute and relative) is rather good, it does appear for both the $O_{2s} - O_{2p}$ and $O_{2p} - O_{2p}$ bands that the

separation between the local and nonlocal contributions should be about 2 eV larger. This could easily be accounted for by somewhat larger values of the two-center repulsion integrals $u(Si_h, O_{2p})$.

C. Summary and conclusion

In both the O KVV and the Si $L_{23}VV$ Auger line shapes there is some evidence that the two-center repulsion integrals u_{mn} should be larger. The "classical" approximation is the Mataga-Nishimoto (MN) approximation [Eq. (13)], but others have recently been suggested. In a recent study by Dewar and Thiel,[35] the Klopman approximation (K) (Ref. 36)

$$u_{mn} = e^2 [R_{mn}^2 + (2e^2/(u_n + u_m))^2]^{-1/2} \qquad (45)$$

was compared with the MN approximation and analytically evaluated two-center integrals. The K integrals were found to be in general agreement with the analytical integrals, the MN integrals generally too small. In the event that the two-center overlaps are known, Huang[15] has proposed the approximation (H)

$$u_{mn} = S_{mn}\tfrac{1}{2}(u_n + u_m) + (1 - S_{mn})e^2/R_{mn} . \qquad (46)$$

Using the overlap integrals evaluated for SiO_2 by Gilbert et al.,[37] we obtain the values given in Table V along with the MN and K integrals.

All three approximations behave properly in the limits $R_{mn} \rightarrow 0$ and $R_{mn} \rightarrow \infty$. It is in the intermediate regions that the approximations differ. On the other hand, it has been argued[38,39] that the appropriate long-range repulsion should behave as $e^2/(kR_{mn})$ where "k" is the dielectric constant of the solid and accounts for the background electron density in solids. In SiO_2 $k \approx 4$, which would significantly decrease the Coulomb repulsion. However, in the short-range region of interest here (nearest neighbor), the macroscopic dielectric constant is probably not appropriate. The results in Table V indicate the MN integrals are smaller than the others in the short-range region. Our interpretation of the experimental Auger line shapes suggest the H or K approximations to be the more appropriate.

In summary, we have in this work elucidated the role of final-state hole-hole correlation ef-

TABLE V. Comparison of approximations for the two-center Coulomb-repulsion integrals in SiO_2. The assumed values of $u(Si_h)$ and $u(O_{2p})$ were 11 and 15 eV, respectively.

Item	Si–O	O–O	Si–Si
R_{mn} (Å)	1.5	2.5	3.0
Overlap $\langle \varphi_m | \varphi_n \rangle$ [a]	0.26	0.063	0.33
Mataga-Nishimoto[b] u_{mn} (eV)	5.5	4.1	3.3
Klopman[c] u_{mn} (eV)	7.7	5.3	4.4
Huang[d] u_{mn} (eV)	10.4	6.3	6.8

[a] From Gilbert et al. (Ref. 37).
[b] Reference 17.
[c] Reference 36.
[d] Reference 15.

fects in Auger line shapes. In the O KLL case, the Auger line shape reveals a strong localization onto a single Si_2O cluster; indeed, it almost appears atomiclike. In the Si $L_{23}VV$ case, the Auger line shape reveals significant contributions from both the local (both holes on the same Si_2O subcluster) and nonlocal (the two holes on neighboring Si_2O subclusters) configurations.

Perhaps most significant in this work is the use of the Auger line shapes to obtain near quantitative information about the hole-hole repulsion magnitudes and bandwidths. In general, the absolute energies of the Auger transitions indicate the magnitude of the one-center integrals; the relative energies and intensities of the local and nonlocal contributions give some information about the two-center repulsion integrals and bandwidths. This suggests that the quantitative interpretation of Auger line shapes might be a useful tool for obtaining important electronic structure information in other insulators and semiconductors and in chemisorbed systems.

ACKNOWLEDGMENTS

[1] D. E. Ramaker, J. S. Murday, N. H. Turner, G. Moore, M. G. Lagally, and J. Houston, Phys. Rev. B 19, 5375 (1979).

[2] D. E. Ramaker and J. S. Murday, J. Vac. Sci. Technol. 16, 510 (1979).

[3] M. K. Bernett, J. S. Murday, and N. H. Turner, J. Electron. Spectrosc. Relat. Phenom. 12, 375 (1977).

[4] P. J. Bassett, T. E. Gallon, M. Prutton, and J. A. D. Matthew, Surf. Sci. 33, 213 (1972).

[5] B. Fischer, R. A. Pollak, T. H. DeStefano, and W. D. Grobman, Phys. Rev. B 15, 3193 (1977).

[6] H. H. Madden, D. M. Zehner, and J. R. Noonan, Phys.

Rev. B 17, 3074 (1978).

[7]D. R. Jennison, Phys. Rev. B 18, 6996 (1978).

[8]E. Antonides, E. C. Janse, and G. A. Sawatzky, Phys. Rev. B 15, 1669 (1977).

[9]J. Hubbard, Proc. R. Soc. London A276, 238 (1963).

[10]P. W. Anderson, Phys. Rev. 109, 1492 (1958).

[11]M. Cini, Solid State Commun. 20, 605 (1976); Phys. Rev. B 17, 2788 (1978).

[12]G. A. Sawatzky, Phys. Rev. Lett. 39, 504 (1977).

[13]R. G. Parr, *The Quantum Theory of Molecular Electronic Structures* (Benjamin, New York, 1963).

[14]D. J. Chadi, R. B. Laughlin, and J. D. Joannopoulos, in *The Physics of SiO$_2$ and Its Interfaces*, edited by S. T. Pantelides (Pergamon, New York, 1978), p. 55.

[15]C. Huang, J. A. Moriarty, and A. Sher, Phys. Rev. B 12, 5395 (1975); 14, 2539 (1976).

[16]B. I. Dunlap, P. Mills, and D. E. Ramaker (unpublished).

[17]N. Mataga and K. Nishimoto, Z. Phys. Chem. (N. F.) 13, 140 (1957).

[18]J. B. Mann, Los Alamos Scientific Laboratory Report No. LASL-3690, 1967 (unpublished).

[19]S. T. Pantelides and W. A. Harrison, Phys. Rev. B 13, 2667 (1976).

[20]J. R. Chelikovsky and M. Schlüter, Phys. Rev. B 15, 4020 (1977).

[21]E. J. McGuire, Phys. Rev. 185, 1 (1969); 2, 273 (1970); 3, 1801 (1971); Phys. Rev. A 3, 587 (1971); Sandia Laboratories Research Report No. SC-RR-710075, 1975 (unpublished).

[22]W. N. Asaad, Nucl. Phys. 66, 494 (1965).

[23]E. J. McGuire, Phys. Rev. A 16, 2365 (1977).

[24]R. W. C. Wyckoff, *Crystal Structures* (Interscience, New York, 1963), Vol. 1.

[25]R. N. Nucho and A. Madhukar, in *The Physics of SiO$_2$ and Its Interfaces*, edited by S. T. Pantelides (Pergamon, New York, 1978), p. 60.

[26]L. Oleari, L. DiSipio, and G. DeMichelis, Mol. Phys. 10, 97 (1966).

[27]D. L. Griscom, J. Non-Cryst. Solids 24, 155 (1977).

[28]I. P. Batra, in *The Physics of SiO$_2$ and Its Interfaces*, edited by S. T. Pantelides (Pergamon, New York, 1978), p. 65.

[29]T. H. DiStefano and D. E. Eastman, Phys. Rev. Lett. 27, 1560 (1971).

[30]H. Ibach and J. E. Rowe, Phys. Rev. B 10, 710 (1974).

[31]C. Sènèvaud, in *The Physics of SiO$_2$ and Its Interfaces*, edited by S. T. Pantelides (Pergamon, New York, 1978), p. 75.

[32]W. N. Assad and E. H. S. Burhop, Proc. Phys. Soc. London 72, 369 (1958).

[33]V. O. Kostroun, M. H. Chen, and B. Crasemann, Phys. Rev. A 3, 533 (1971).

[34]B. W. Shore and D. H. Menzel, *Principles of Atomic Spectra* (Wiley, New York, 1968).

[35]M. J. S. Dewar and W. Thiel, Theor. Chim. Acta 46, 89 (1977).

[36]G. Klopman, J. Am. Chem. Soc. 86, 4550 (1964).

[37]T. L. Gilbert, W. J. Stevens, H. Schrenk, M. Yoshimine, and P. S. Bagus, Phys. Rev. B 8, 5977 (1973).

[38]C. Kittel, *Introduction to Solid State Physics*, 4th ed. (Wiley, New York, 1971), p. 373.

[39]N. F. Mott and E. A. Davis, *Electronic Processes in Non-crystalline Materials* (Oxford University Press, Oxford, 1971), p. 132.

[40]D. J. Chadi and M. L. Cohen, Phys. Status Solidi B 68, 405 (1975).

[41]K. Schmidtal, Surf. Sci. 77, 523 (1978).

[42]V. M. Bermudez and V. H. Ritz, Phys. Rev. B 20, 3446 (1979).